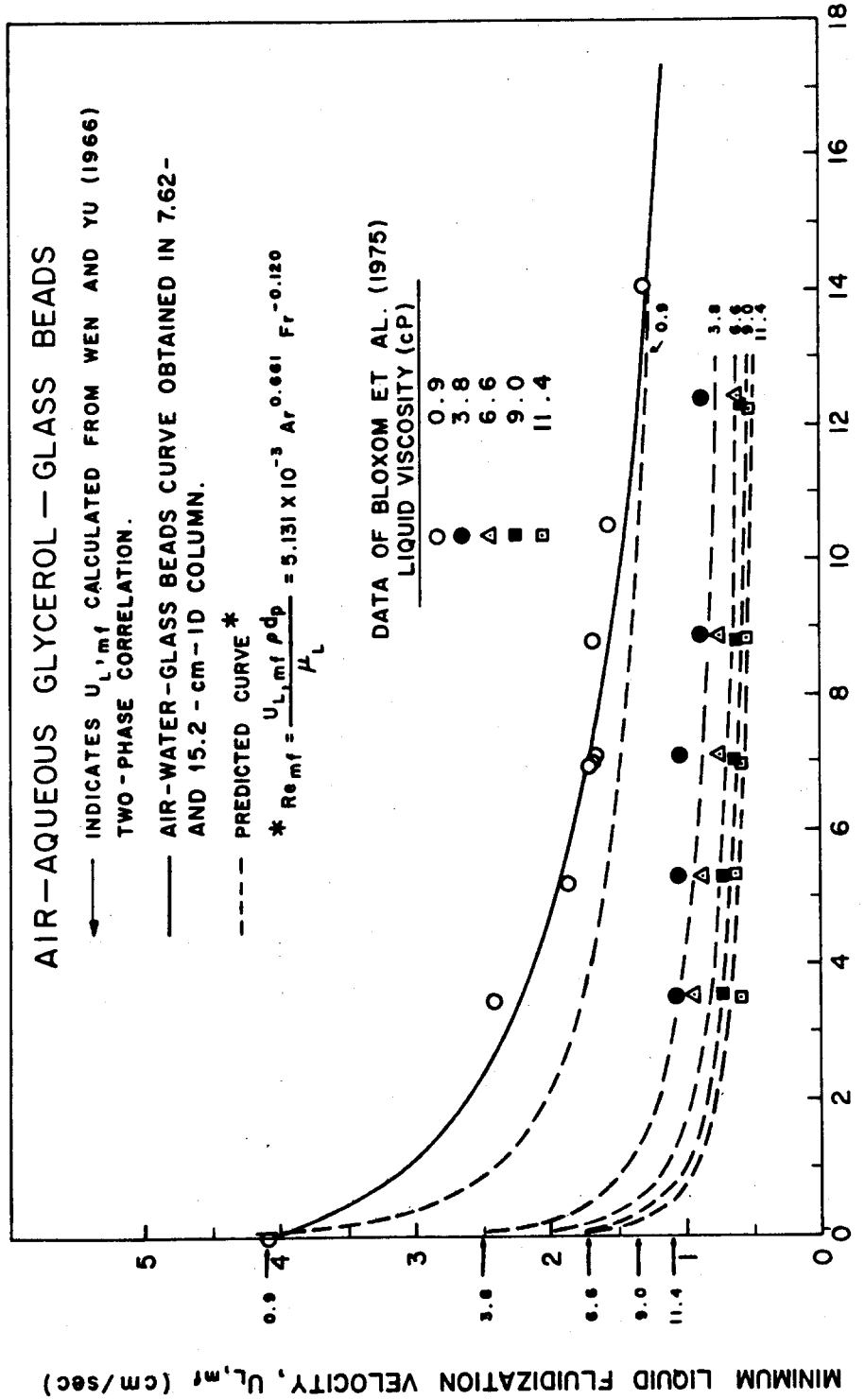

Fig. 2.36. Effect of liquid viscosity on the predicted vs experimental MF data.

Overall phase holdups. Measurements of the overall solid holdup, $\bar{\varepsilon}_S$, from this study were combined with 1355 points from the literature[38-47] to develop the following dimensional correlation in centimeter-gram-second (cgs) units:

$$1 - \bar{\varepsilon}_S = aU_L^{\ b}U_G^{\ c}(\rho_S - \rho_L)^d d_p^{\ e}\mu_L^{\ f}D_c^{\ g} , \qquad (8)$$

where D_c = column diameter and the constants and their 95% confidence limits are

$a = 0.371 \pm 0.013$, $e = -0.268 \pm 0.008$,

$b = 0.271 \pm 0.008$, $f = 0.055 \pm 0.006$,

$c = 0.041 \pm 0.004$, $g = -0.033 \pm 0.010$.

$d = -0.316 \pm 0.008$,

Figure 2.37 presents the results of this study in a parity plot. The equation was based on a total of 2381 data points and has a correlation coefficient of 0.87 and an F-value of 1178. Although the considerable data scatter is evident, these correlations show considerable improvement over previous ones presented in the literature.

Combining the data for overall gas holdup, $\bar{\varepsilon}_G$, with 169 data points available from the literature,[38,41-43,45] we developed the following correlation:

$$\bar{\varepsilon}_G = aU_G^{\ b}d_p^{\ c}D_c^{\ d} , \qquad (9)$$

where the constants and their 95% confidence limits are

$a = 0.048 \pm 0.008$, $c = 0.168 \pm 0.046$,

$b = 0.720 \pm 0.021$, $d = -0.125 \pm 0.067$.

Again, cgs units are used for each parameter. Equation (9) is based on a total of 913 points and has a correlation coefficient of 0.93 and an

ORNL DWG 78-403

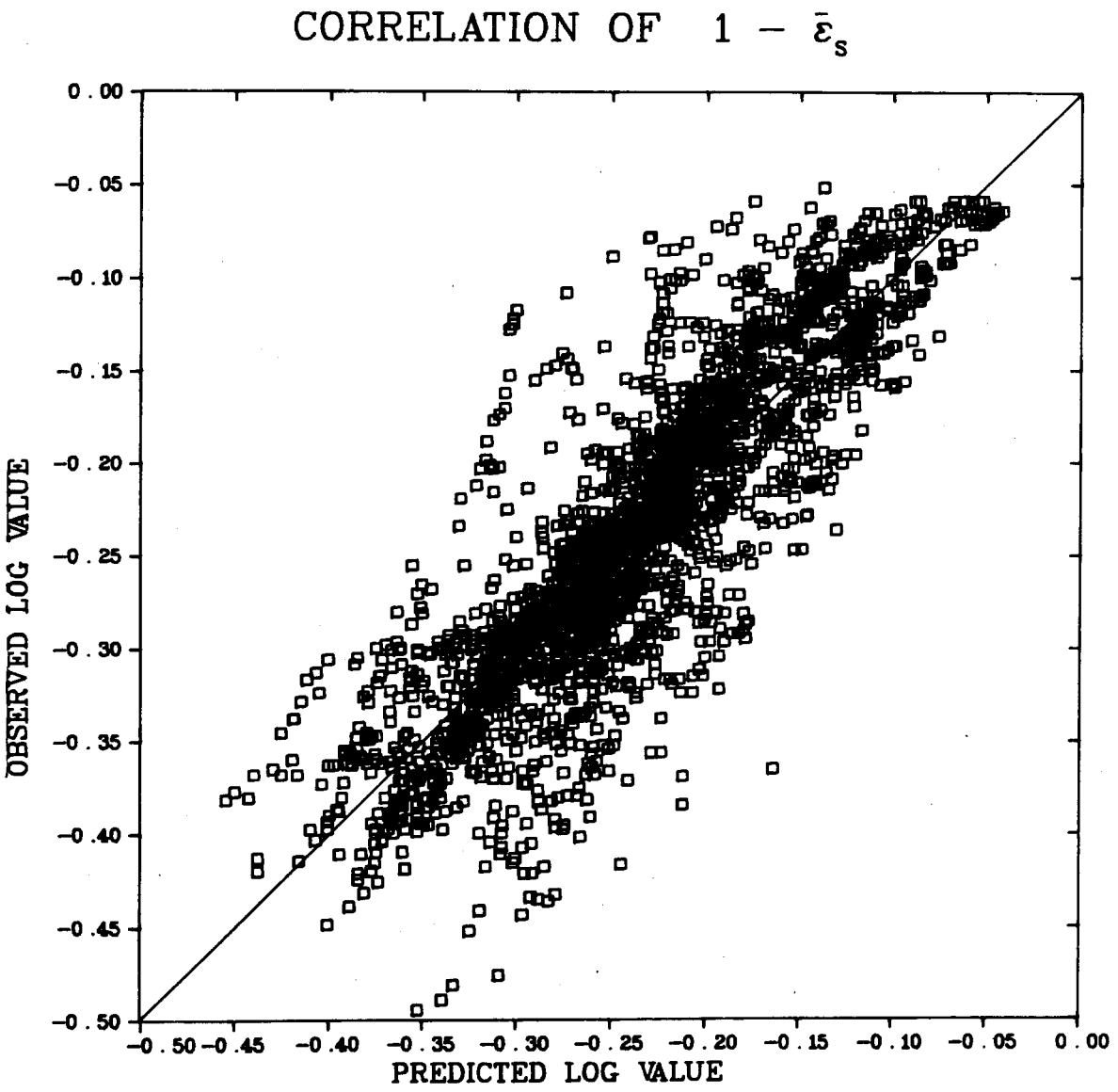

Fig. 2.37. Predicted vs experimental overall solid holdup values.

F-value of 1793. The results of this correlation, which are shown in a parity plot in Fig. 2.38, represent a significant improvement in existing correlations, principally because this study has greatly increased the range of conditions studied.

Local holdups. The local holdup versus column position shown previously[1] clearly indicated that each of the holdups is approximately constant in two regions: the lower portion of the bed and the gas-liquid region above the bed. The transition region between these two extremes depends on the gas velocity and the physical characteristics of the solid particles. An inflection point was observed on each curve with a spread about that point proportional to the width of the transition region. If each curve were differentiated, these two parameters would correspond to the mean and standard deviation of the normalized Gaussian curves. An error function was used to fit the gas- and solid-holdup curves, and the liquid-holdup curve was determined as the residual of the following:

$$\varepsilon_G + \varepsilon_L + \varepsilon_S = 1 \ , \tag{10}$$

where

ε = phase holdup

and subscripts

G = gas phase,

L = liquid phase,

S = solid phase.

Use of the error function was essentially equivalent to use of the probability integral, since the two are related by the following:

$$\mathrm{erf}(x) = 2\Phi(\sqrt{2}x) \ , \tag{11}$$

ORNL DWG 78-404

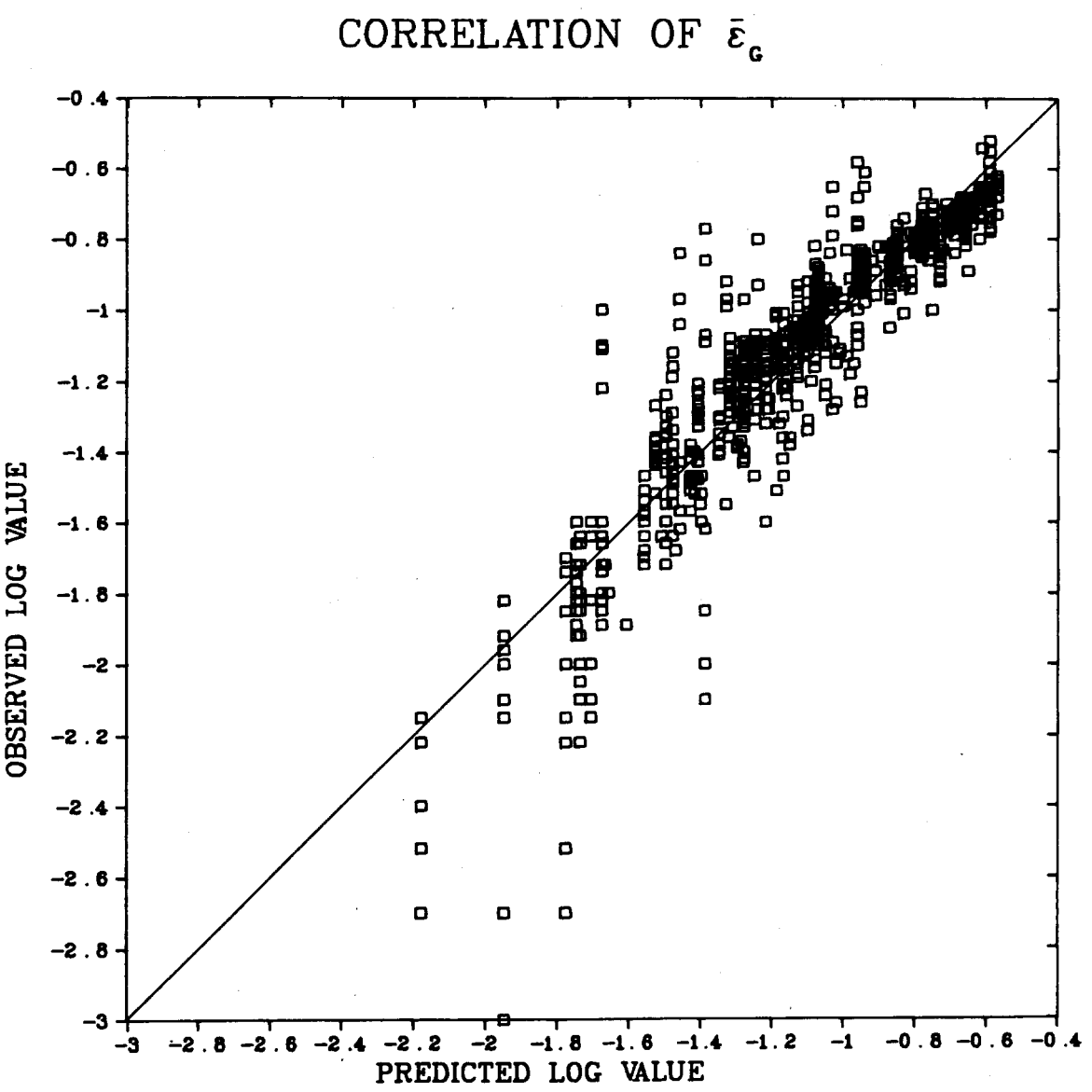

Fig. 2.38. Predicted vs experimental overall gas holdup values.

where

$\text{erf}(x)$ = error function,

$$\frac{2}{\sqrt{\pi}} \int_0^x e^{-z^2} \, dz \ ,$$

$\Phi(x)$ = probability integral,

$$\frac{1}{\sqrt{2\pi}} \int_0^x e^{-w^2/2} \, dw \ .$$

Thus the gas holdup curves were fitted by the following:

$$\varepsilon_G = [(P_G - 1)/-2]\varepsilon_G''' + [(P_G + 1)/2]\varepsilon_G'' \ , \tag{12}$$

where

$'''$ = three-phase region of the column,

$''$ = two-phase (gas-liquid) region of the column,

$$P_G = \text{erf}\,[(h - I_G)/\sigma_G] \ , \tag{13}$$

h = axial column position,

I = inflection point in local holdup versus height curve,

σ = standard deviation in local holdup versus height curve.

The solid holdup was fitted similarly using the error function and the knowledge that the solid holdup in the gas-liquid region of the column is zero:

$$\varepsilon_S = [(P_S + 1)/2]\varepsilon_S''' \ , \tag{14}$$

where

$$P_S = -\text{erf}\,[(h - I_S/\sigma_S] \ . \tag{15}$$

The liquid holdup at each point was obtained from the residual to Eq. (10).

Thus, knowledge of seven parameters — ε_G''', ε_G'', ε_S''', σ_S, σ_G, I_S, and I_G — allows description of each of the phase holdups at all axial

column positions. Figure 2.39 shows an example of such a fit. For the example system shown, the seven parameters were

$\varepsilon_G'''' = 0.072$, $I_G = 45.7$ cm,

$\varepsilon_G'' = 0.129$, $\sigma_S = 2.83$ cm,

$\varepsilon_S'''' = 0.551$, $\sigma_G = 2.64$ cm.

$I_S = 45.7$ cm,

Treatment of the experimental data in this way and correlation of the seven parameters with fluid and solid properties and experimental conditions using least-squares multiple linear regression analysis resulted in a predictive equation for each parameter.

The gas holdup in the three-phase region of the column was successfully correlated by the following:

$$\varepsilon_G'''' = a[U_G^5(\rho_S - \rho_L)U_L g\sigma_{LV}]^b \quad , \tag{16}$$

where σ_{LV} = interfacial tension and constants a and b and their 95% confidence limits are 0.159 ± 0.008 and 0.150 ± 0.006 respectively. Equation (16), shown as a parity plot in Fig. 2.40, had a correlation coefficient of 0.89 and an F-value of 2155 and was based on a total of 555 points.

Data on the gas holdup in the two-phase portion of the column (above the bed) were used to develop the following dimensionless correlation:

$$\varepsilon_G'' = a[U_G^4(\rho_S - \rho_L)/g\sigma_{LV}]^b \quad , \tag{17}$$

where constants a and b and their 95% confidence limits are 0.237 ± 0.010 and 0.185 ± 0.006 respectively. Equation (17) had a correlation coefficient of 0.93 and an F-value of 4266. The 634 points on which it was based are shown as a parity plot in Fig. 2.41. Most of the scatter shown in the

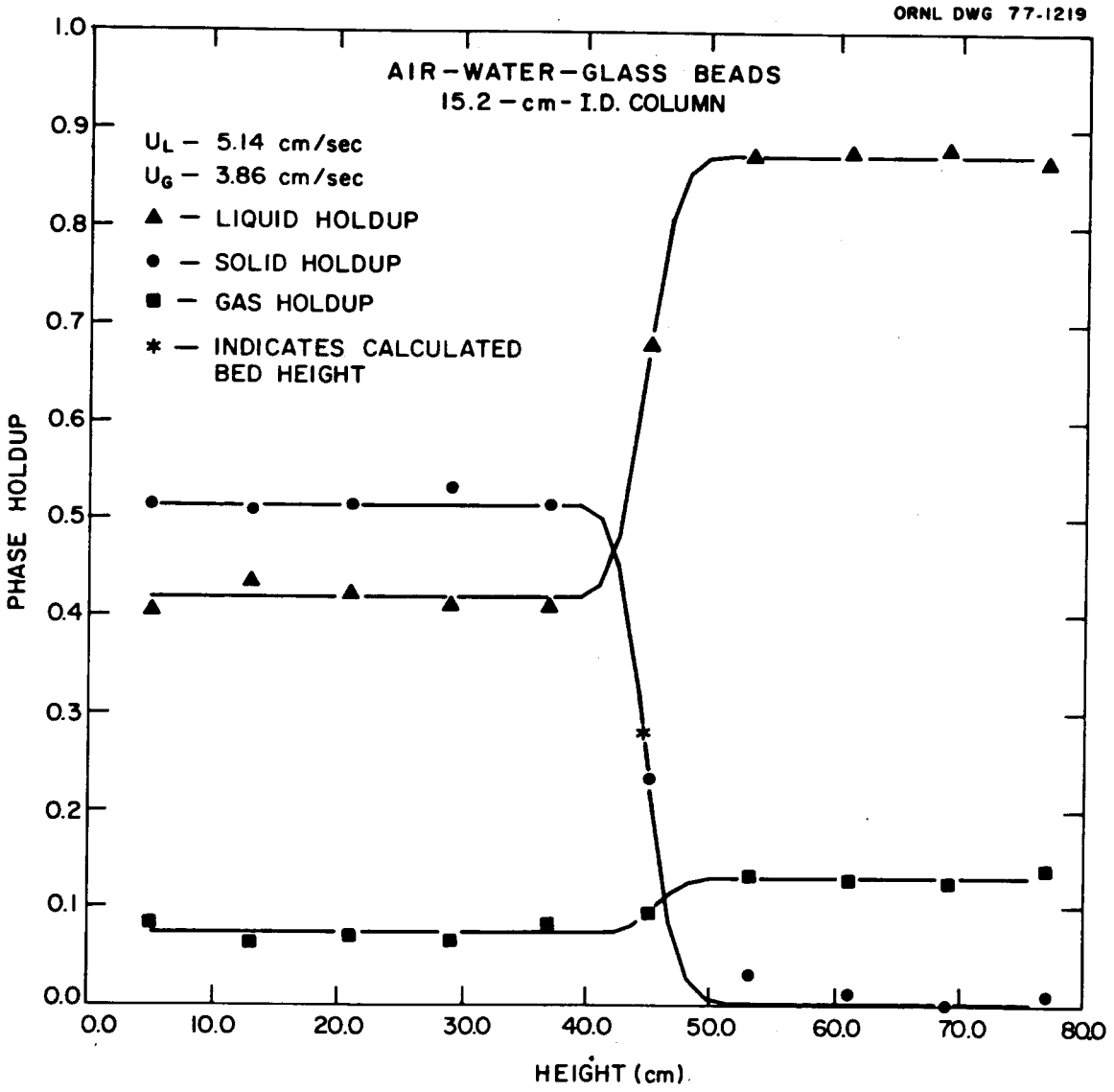

Fig. 2.39. Fit of local holdup profiles for the air-water-glass beads.

ORNL DWG 78-392R

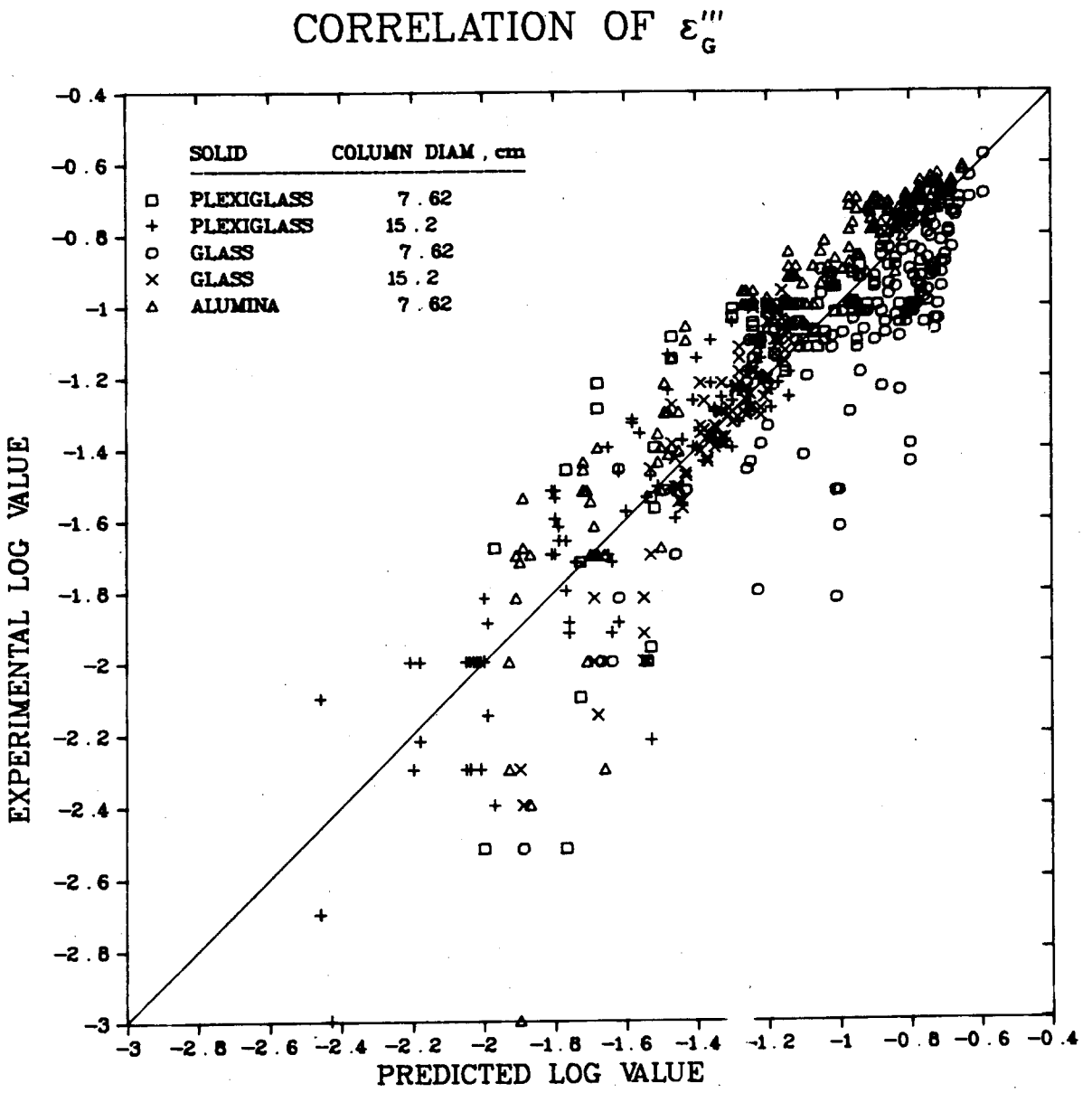

Fig. 2.40. Predicted vs experimental values of the gas holdup in the three-phase region.

ORNL DWG 78-393

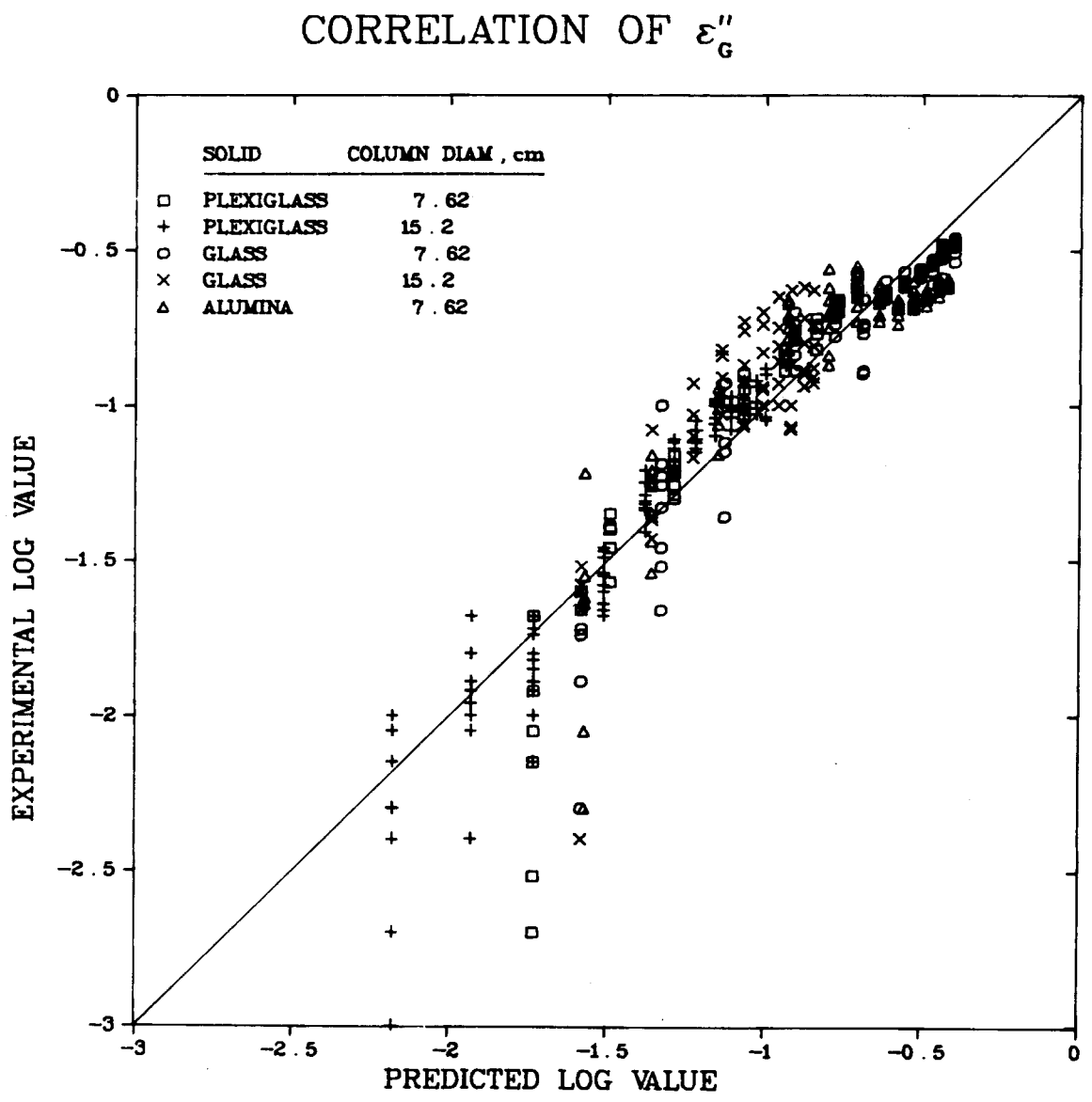

Fig. 2.41. Predicted vs experimental values of the gas holdup in the two-phase region.

figure results from the low-density (and low-density-difference) plexiglass data.

The solid holdup in the bed was correlated as follows:

$$1 - \varepsilon_S''' = aAr^b Re_L^c (H/H_o)^d \ , \tag{18}$$

where

$Re_L = \rho_L U_L d_p / \mu_L$,

H = expanded bed height (i.e., the height at which the pressure gradients in the two- and three-phase regions intersect),

H_o = static bed height,

and the constants and their 95% confidence limits are

$a = 1.990 \pm 0.273$, $c = 0.197 \pm 0.011$,

$b = -0.178 \pm 0.012$, $d = 0.298 \pm 0.018$.

Figure 2.42 shows a parity plot of Eq. (18), which has a correlation coefficient of 0.95 and an F-value of 2529 and was based on 762 points.

Equation (18) requires a value for the expanded bed height; this was also correlated with the system properties and resulted in the following equation:

$$H/H_o = aFr_G^b Re_L^c Ar^d [(\rho_S - \rho_L)/\rho_L]^e \ , \tag{19}$$

where the constants and their 95% confidence limits are

$a = 10.483 \pm 5.7$, $d = -0.295 \pm 0.039$,

$b = 0.069 \pm 0.005$, $e = -0.305 \pm 0.027$.

$c = 0.429 \pm 0.025$,

Equation (19), based on a total of 706 points, had a correlation coefficient of 0.90 and an F-value of 762; it is shown as a parity plot in Fig. 2.43. Again, most of the scatter occurs in the data from the plexiglass solids.

ORNL DWG 78-394

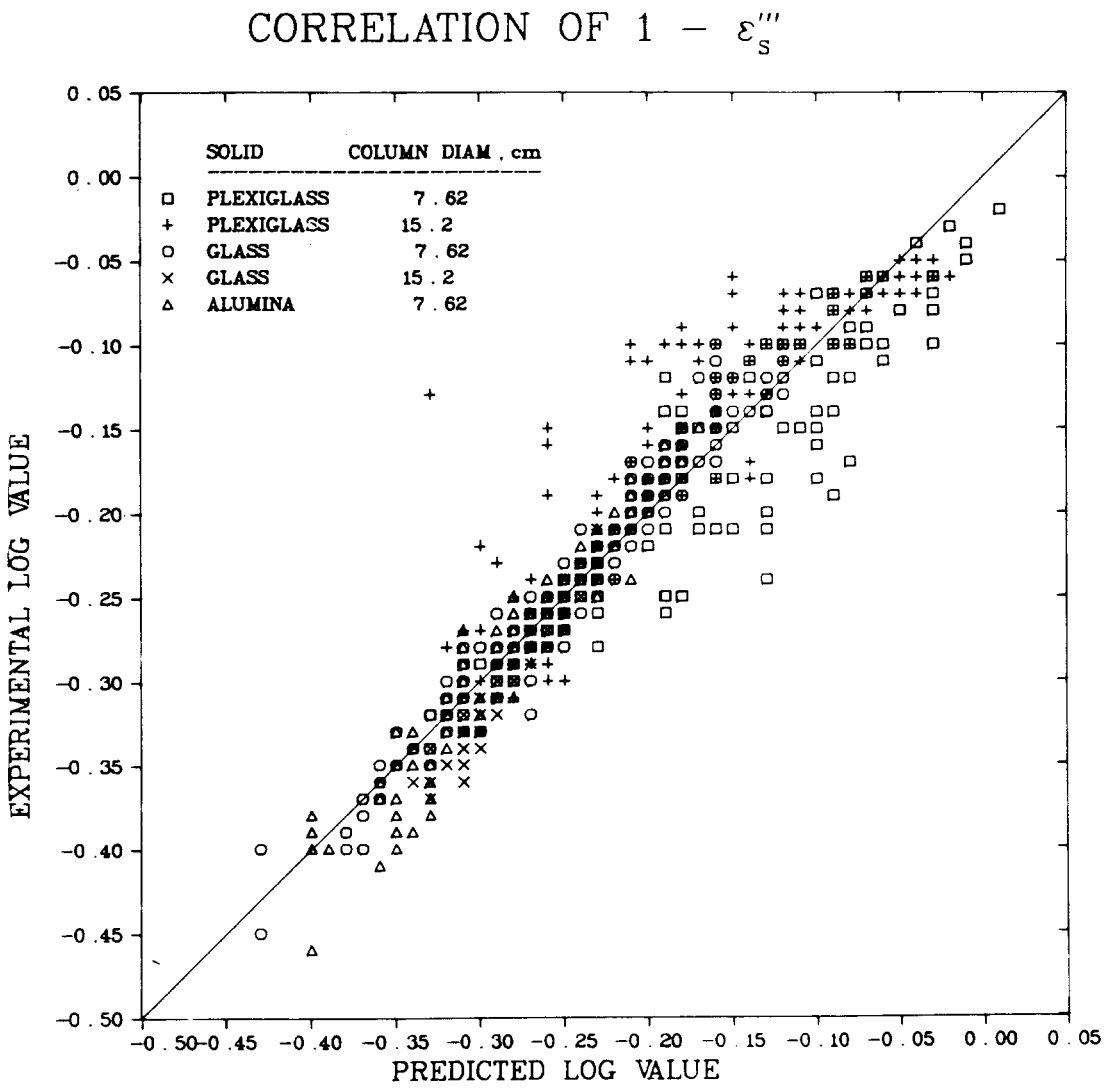

Fig. 2.42. Predicted vs experimental values of the solid holdup in the three-phase region.

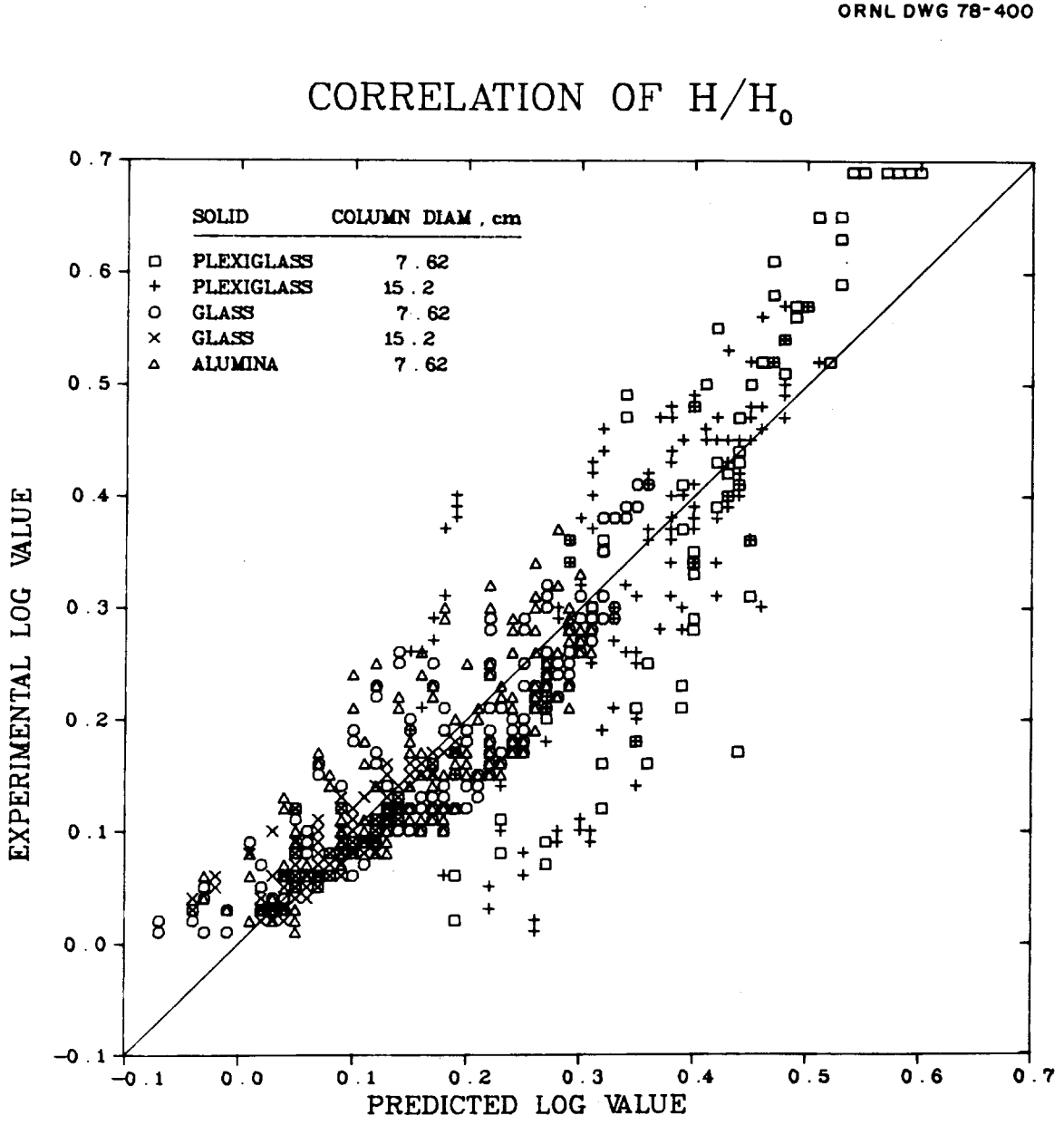

Fig. 2.43. Predicted vs experimental expanded bed height values.

The inflection point in the solid holdup curve followed the calculated bed height fairly closely and could be correlated by the following:

$$I_S = aU_G^{\,b}U_L^{\,c}D_c^{\,d}H^e \ , \qquad (20)$$

where the constants and their 95% confidence limits are

$a = 2.354 \pm 0.440$, $d = 0.061 \pm 0.031$,

$b = 0.017 \pm 0.008$, $e = 0.628 \pm 0.045$.

$c = 0.247 \pm 0.017$,

Equation (20), shown as a parity plot in Fig. 2.44, had a correlation coefficient of 0.92 and an F-value of 875 and was based on a total of 689 points. The agreement is very good except for the plexiglass data.

Similarly, the inflection point in the gas holdup curve followed that in the solid holdup curve, yielding the following correlation:

$$I_G/H_o = a(\rho_S - \rho_L)^b d_p^{\,c} D_c^{\,d} I_S^{\,e} \ , \qquad (21)$$

where the constants and their 95% confidence limits are

$a = 0.027 \pm 0.006$, $d = 0.170 \pm 0.045$,

$b = -0.250 \pm 0.026$, $e = 0.875 \pm 0.049$.

$c = -0.145 \pm 0.123$,

Equation (21) is based on a total of 635 points, and the results are shown as a parity plot in Fig. 2.45. The correlation coefficient was 0.849 and the F-value was 408.

The standard deviations in the local holdups versus height curves were the most difficult parameters to measure since a slight variation in the local holdup affected the standard deviation considerably; this variation would make the standard deviations more difficult to correlate. The

ORNL DWG 78-396

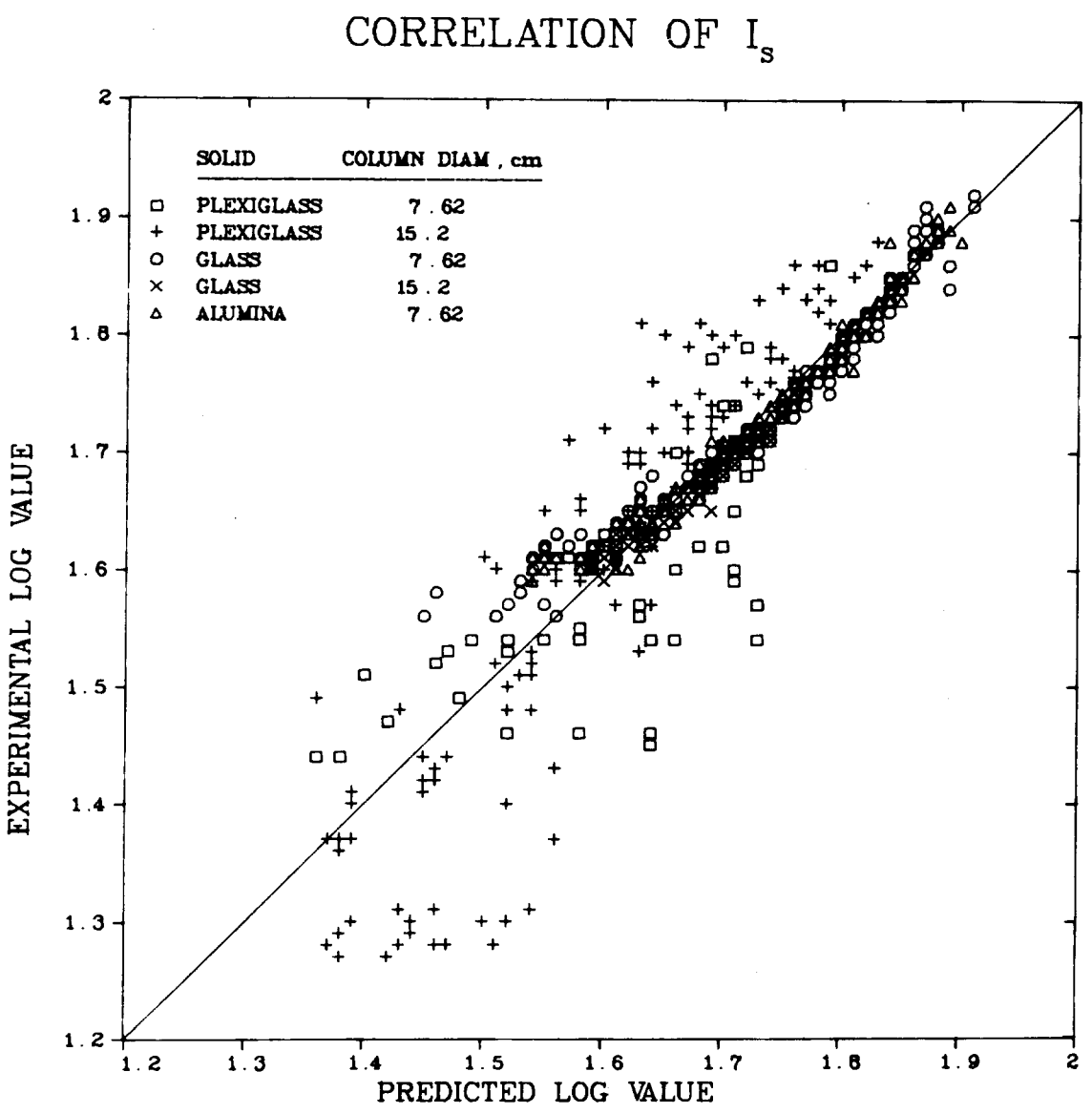

Fig. 2.44. Predicted vs experimental values of the inflection points of the solid holdup curve.

ORNL DWG 78-395

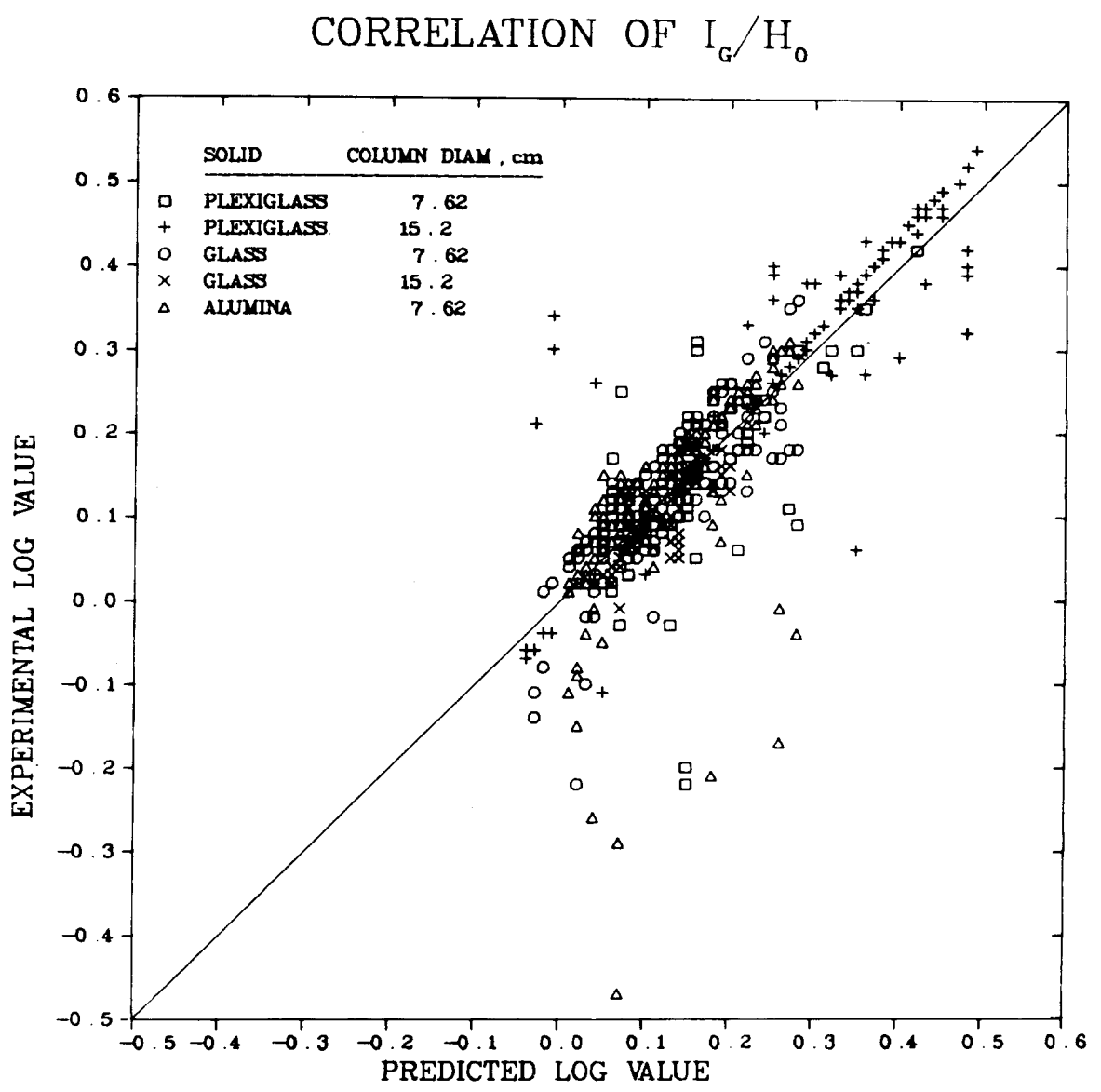

Fig. 2.45. Predicted vs experimental values of the inflection points of the gas holdup curve.

standard deviation in the solid holdup curve can be estimated from the following correlation:

$$\sigma_S/H_o = aC_D^{\,b}Fr_H^{\,c} \quad , \tag{22}$$

where

C_D = drag coefficient = $(\rho_S - \rho_L)d_p/\rho_L U_G^{\,2}$,

Fr_H = Froude number based on bed height = $U_G^{\,2}/gH$,

and the constants and their 95% confidence limits are

$a = 5.510 \times 10^{-6} \pm 3.3 \times 10^{-6}$,

$b = -1.015 \pm 0.052$,

$c = -0.840 \pm 0.048$.

Figure 2.46 presents Eq. (22) as a parity plot. The equation had a correlation coefficient of 0.84 and an F-value of 752 and was based on a total of 635 points. Although the data scatter was considerable, the data are useful and important because they represent the only data and the only correlation which attempts to describe axial variation in column properties.

Unfortunately, the standard deviation in the gas holdup curve was even more difficult to correlate than σ_S. A very rough estimate of σ_G can be obtained from the following correlation:

$$\sigma_G/H_o = a(\varepsilon_G'' - \varepsilon_G''')^b(\rho_S - \rho_L)^c d_p^{\,d} H^e \sigma_S^{\,f} \quad , \tag{23}$$

where the constants and their 95% confidence limits are

$a = 0.005 \pm 0.004$, $\quad d = -0.861 \pm 0.461$,

$b = 0.132 \pm 0.061$, $\quad e = 0.693 \pm 0.242$,

$c = -0.362 \pm 0.094$, $\quad f = 0.429 \pm 0.090$.

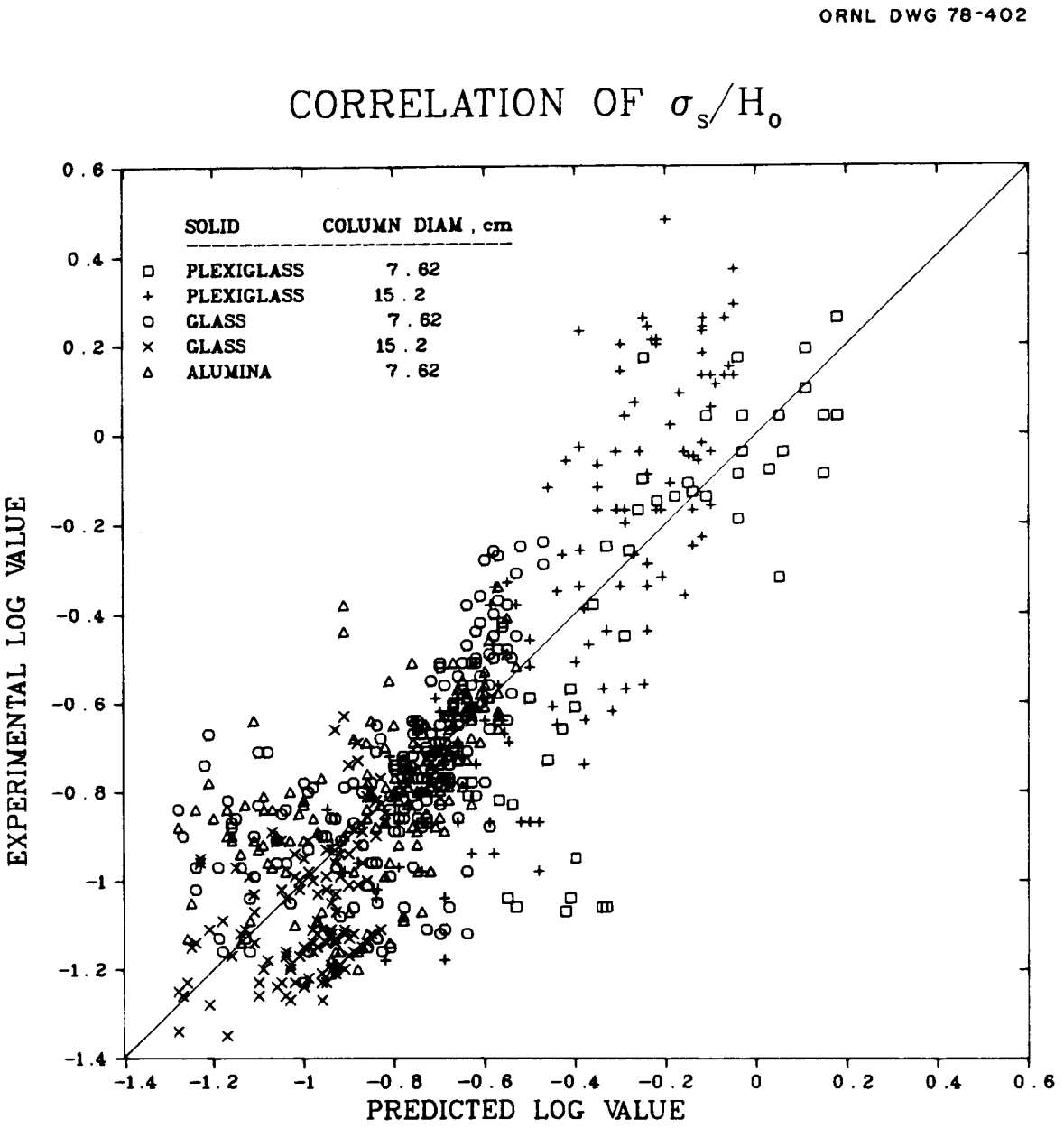

Fig. 2.46. Predicted vs experimental values of the standard deviations of the solid holdup curve.

Equation (23), based on a total of 609 points, had a correlation coefficient of only 0.66 and an F-value of only 93. The parity plot, shown in Fig. 2.47, illustrates the large variation between the measured and calculated values of σ_G. Much of the variation was due to the two plexiglass-bead systems. With their small solid-liquid density difference, these beads made the pressure gradient, and thus the holdups, difficult to measure; hence, there was a large amount of scatter in the parity plot.

Reduction of parameters. Because of the scatter in the experimental data, using the different parameters to describe the local holdup of each phase was difficult to justify. In the fitting of the local holdup versus height curves, the inflection points and standard deviations of the gas and solid phases were similar. Thus, it might be more appropriate to estimate the inflection point and the standard deviation in the gas-phase curves by equating them to the predicted solid-phase values rather than by using Eqs. (21) and (23).

The inflection points in the gas-holdup curves are shown in Fig. 2.48 plotted against the solid-holdup inflection points. Similarly, the standard deviations in the gas-holdup curves are plotted against those in the solid holdup curves as shown in Fig. 2.49. Although a good deal of scatter is evident in Fig. 2.48 and, especially, in Fig. 2.49, data from Figs. 2.45 and 2.47, representing least-square fits, are also scattered. In fact, because of the scatter in the correlated fits, it is recommended that both the inflection point and the standard deviation of each of the three holdup curves be estimated by a single equation. For the standard deviation in the holdup curves, Eq. (22) should be used.

For the inflection point in the holdup curves, a further simplification can be made. As mentioned previously, the inflection point in the

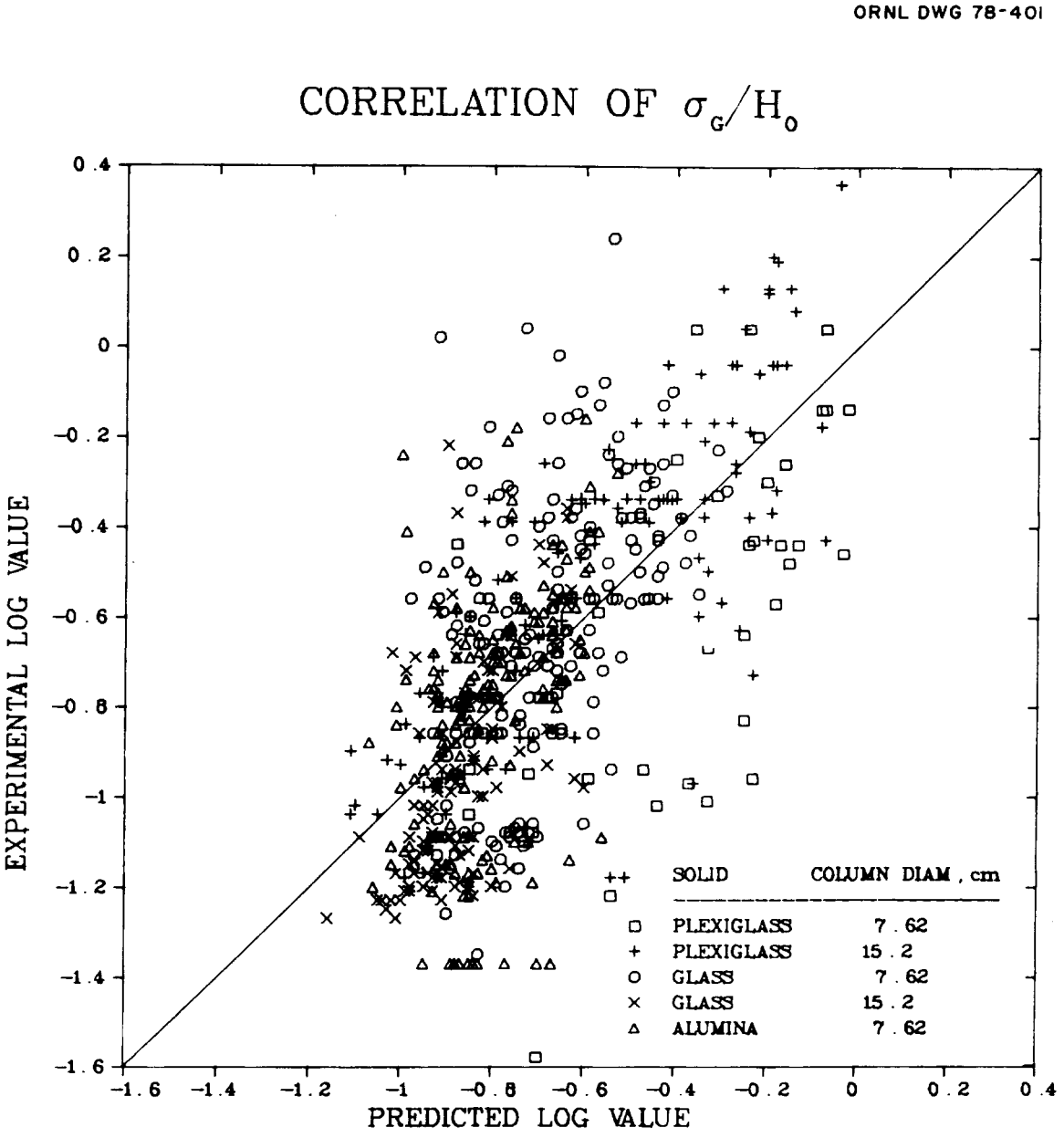

Fig. 2.47. Predicted vs experimental values of the standard deviations of the gas holdup curve.

ORNL DWG 78-397

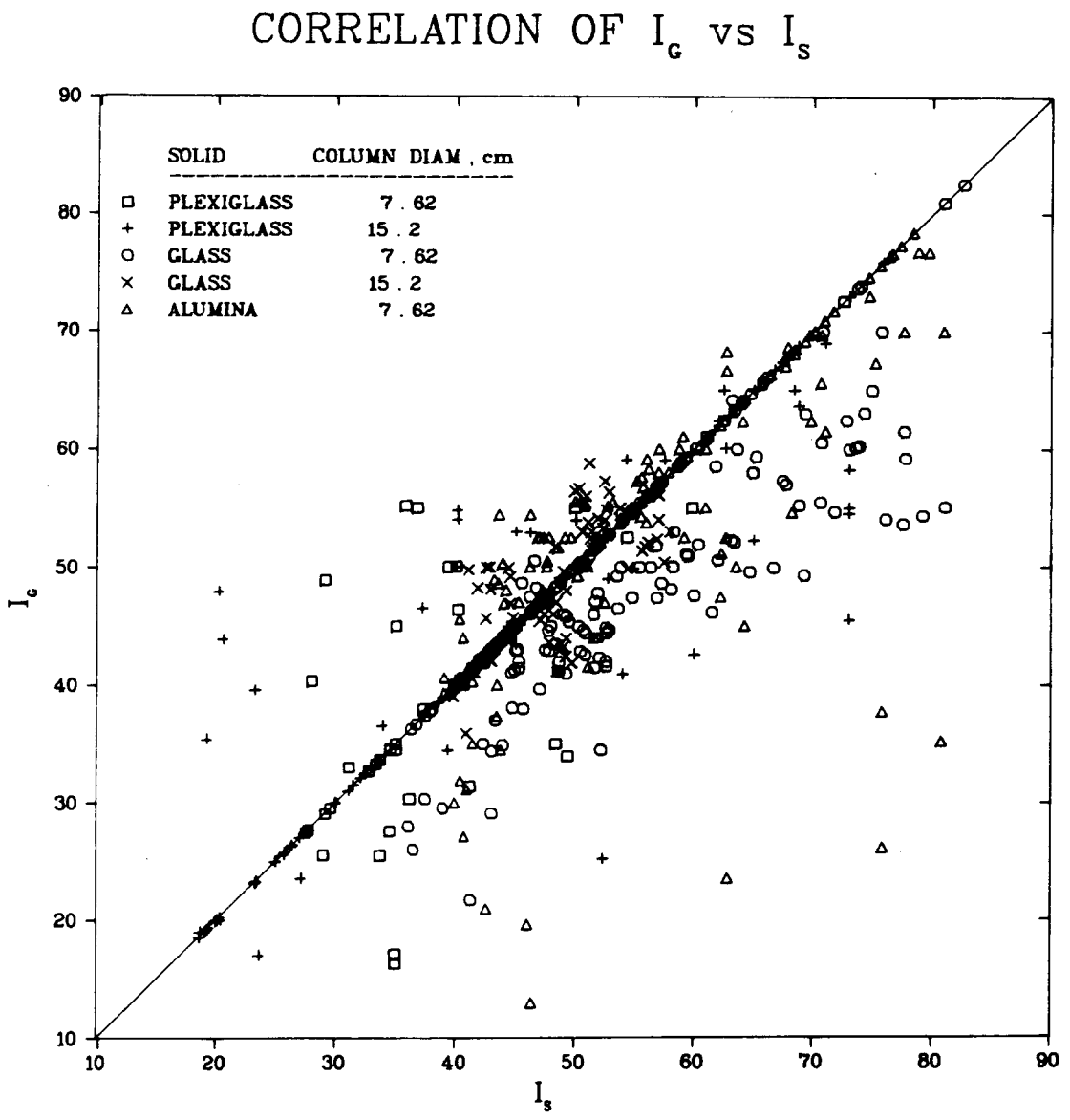

Fig. 2.48. Inflection points of the gas holdup curve vs inflection points of the solid holdup curve.

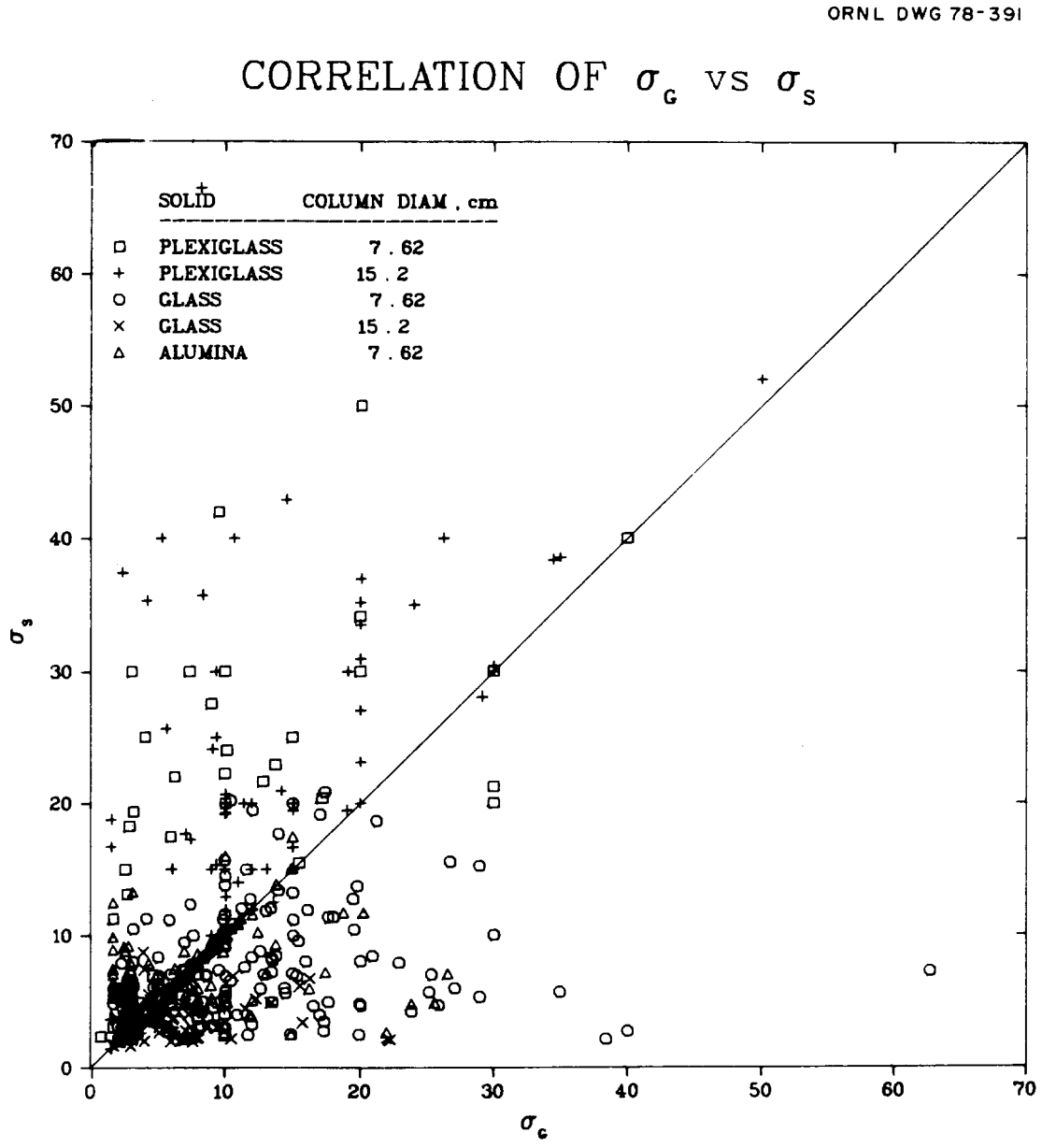

Fig. 2.49. Standard deviations of the gas holdup curve vs standard deviations of the solid holdup curve.

solid holdup curve followed the calculated bed height closely. The two parameters are shown plotted against each other in Fig. 2.50. The agreement between the two is quite good, as expected, since the calculated bed height represents that height in the column of an equivalent homogeneous bed. Disagreements occur chiefly for beds of plexiglass beads, and particularly for highly expanded beds.

Figure 2.51 presents an example of an expanded bed of plexiglass beads. For this specified set of conditions, the concentration of solids dropped very gradually to zero, giving a solid-holdup inflection point of 36 cm. However, the pressure gradient over the two- and three-phase regions yielded a calculated bed height of 49 cm. As mentioned previously, the low solid-liquid density difference of the plexiglass beads made calculation of the bed heights and pressure drops subject to potentially larger errors than those associated with the other solids studied. Thus, with the possible exception of very low solid-liquid density difference systems, Eq. (19) should be used to predict both the expanded bed heights and the inflection points in the three holdup curves.

In summary, it is recommended that the following dimensionless correlations be used to construct phase-holdup curves versus column position curves: (1) that Eqs. (16)-(18) be used to estimate the gas and solid holdups in the two- and three-phase regions; (2) that Eq. (19) be used to determine the inflection point in each of the three holdup curves; and (3) that Eq. (22) be used to determine the standard deviation in each of the three holdup curves.

Centimeter-gram-second units were used in all of the parameters employed in these correlations [Eqs. (16)-(23)]. The correlations were

ORNL DWG 78-398

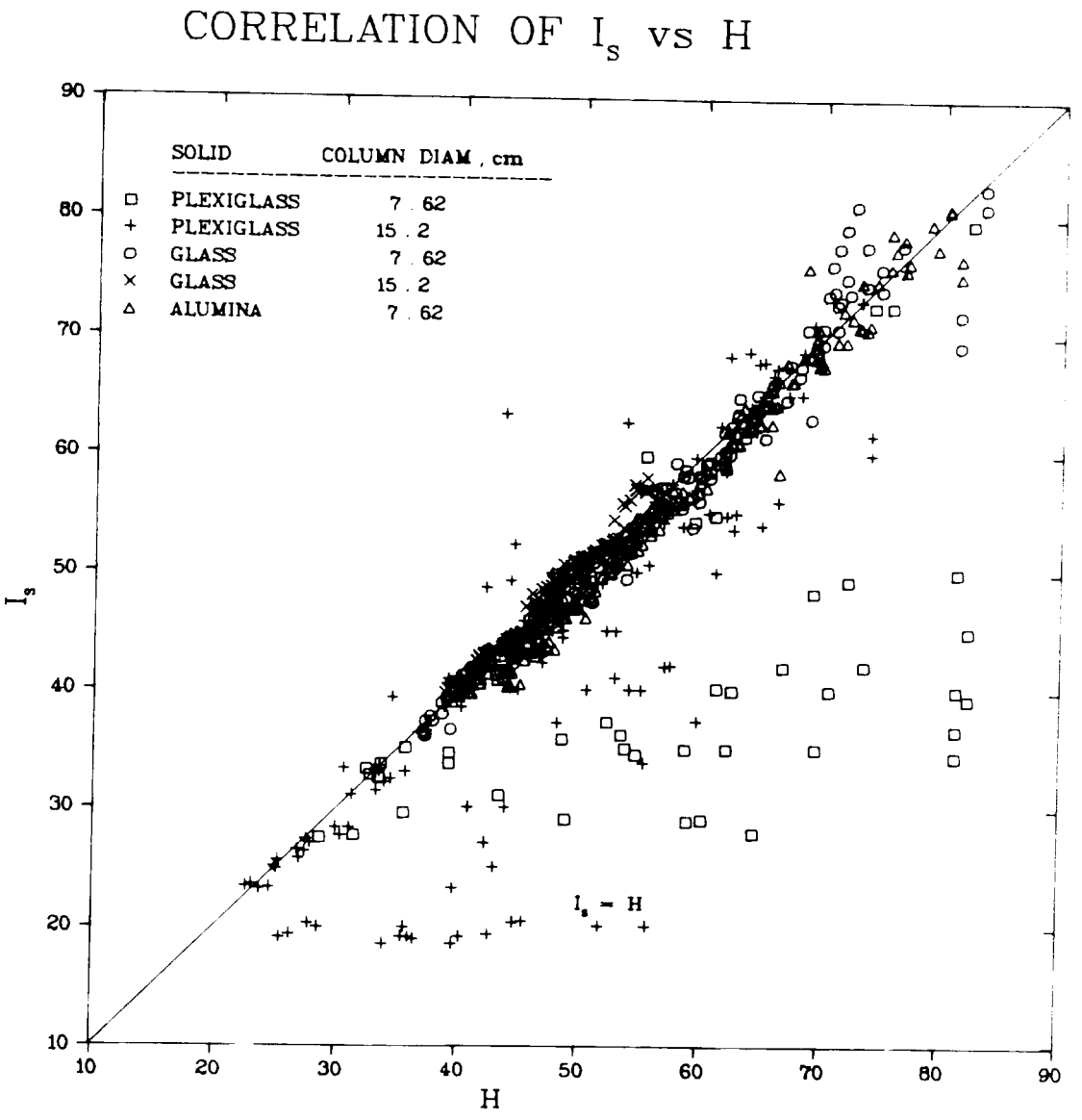

Fig. 2.50. Inflection points of the solid holdup curve vs calculated bed heights.

ORNL DWG 78-405

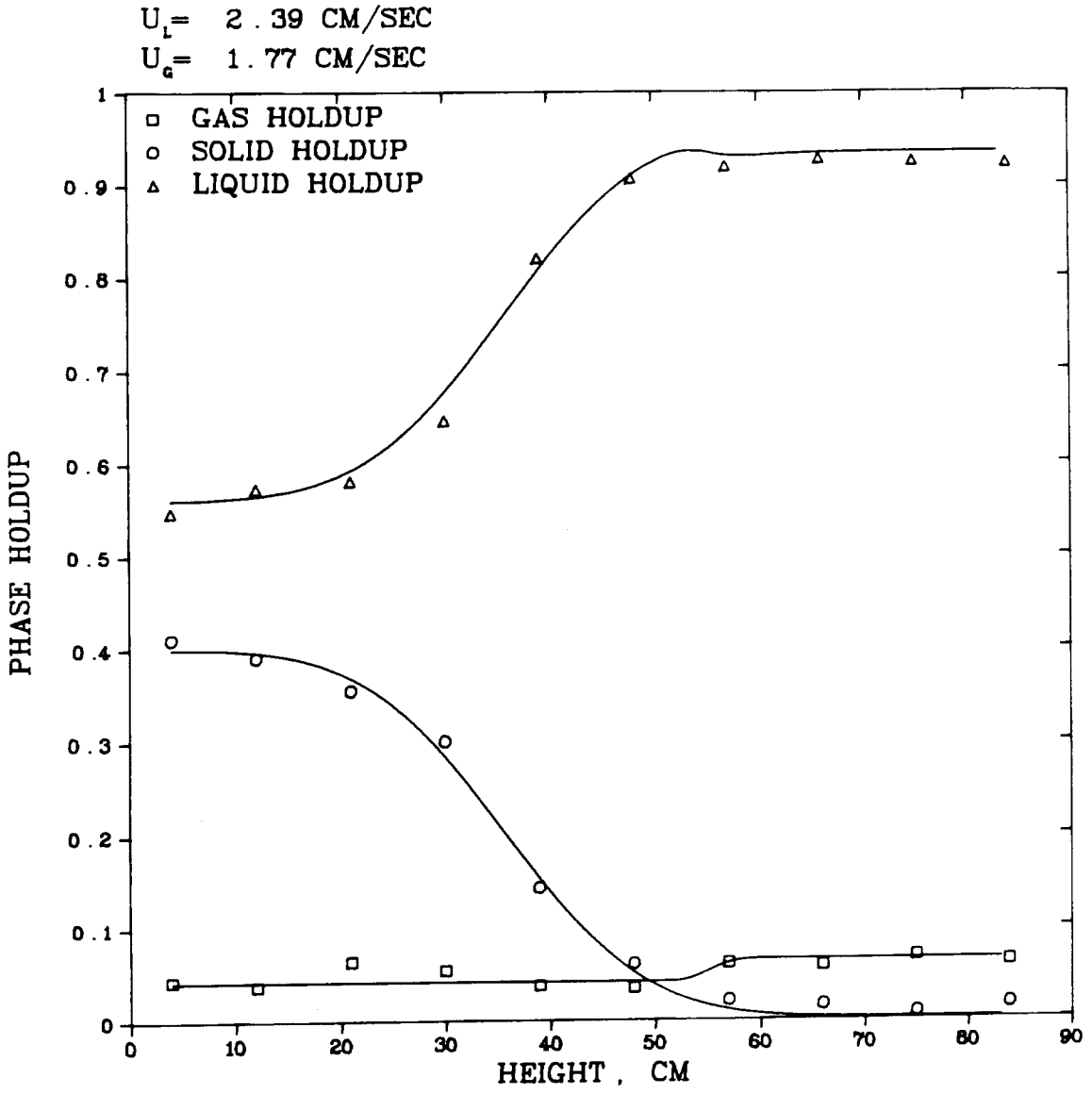

Fig. 2.51. Axial variation of phase holdups in a bed of plexiglass beads.

based on a varying number of total points, depending on how many of the points used were zero (i.e., ε_G''', ε_G'', σ_G, and I_G) and how many were associated with zero gas-flow rates. Such points could not be logarithm transformed and hence could not be used in the multiple linear regression analysis. Also, a number of experimental conditions were used such that the bed height was above the highest manometer tap. For such conditions, the transition between the three- and two-phase regions could not be determined, so only the solid holdup was measured.

2.5.4 Conclusions

The minimum gas and liquid velocities required to fluidize various types of solids have been determined and correlated as a function of particle size, particle density, and liquid viscosity. No effect of the initial bed height or column diameter was found.

Overall phase holdups determined from a homogeneous bed model were combined with similarly determined literature data to yield correlations for the overall solid and gas holdups. The overall solid holdup was primarily a function of the liquid velocity, solid-liquid density difference, and the particle diameter; it varied proportionally with the latter two parameters and inversely with the liquid velocity. The overall gas holdup was primarily a function of the gas velocity and was almost proportional to it.

Using the seven parameters determined from the local gas and solid holdup profiles, it was possible to fit each of the holdup versus column height curves. Use of the dimensionless correlations of just five of these parameters — ε_G''', ε_G'', ε_S''', σ_S, and H — should give a reactor designer more information concerning important phase distributions than that available

from the simpler homogeneous bed model and thereby aid in the rational design of reactors in which local conditions throughout the bed must be considered.

2.6 References for Section 2

1. J. S. Watson and S. D. Clinton (compilers), Advanced Technology Sect. Semiannu. Prog. Rep. for the Period Sept. 1, 1976, to Mar. 31, 1977, Vol. 2: Engineering Science Programs, ORNL/TM-6012/V2 (December 1978).

2. C. D. Scott, et al., Experimental Engineering Sect. Semiannu. Prog. Rep. (Excluding Reactor Programs), Sept. 1, 1975, to Feb. 29, 1976, ORNL/TM-5533 (July 1977).

3. D. Bradley, The Hydroclone, pp. 63-88, Pergamon, New York, 1965.

4. T. Trinh, G. G. Monge, and W. A. Chrusciel, Efficiency of Particle Removal from Viscous Liquids with a Hydroclone, ORNL/MIT-237 (October 1976).

5. D. Bradley, A Contribution to the Theory of the Hydraulic Cyclone and Data on the Performance of Small Diameter Cyclones, Part III, United Kingdom Atomic Energy Authority, AERE-R3146 (1959).

6. G. M. Chaplin, A Mathematical Description of Hydroclone Dynamics, (Thesis), University of Arizona (1972).

7. J. S. Watson and S. D. Clinton (compilers), Experimental Engineering Sect. Semiannu. Prog. Rep. Mar. 1, 1976, to Aug. 31, 1976. Vol. 3: Engineering Science Programs, ORNL/TM-5865/V3 (June 1978).

8. J. G. Van Kooy, "The Influence of the Reynolds Number on the Operation of a Hydroclone," p. 70 in Cyclones in Industry, Elsevier, Amsterdam, The Netherlands, 1961.

9. E. J. W. Verwey and J. T. G. Overbeek, Theory of the Stability of Lyophobic Colloids, Elsevier, New York, 1948.

10. Ayao Kitahara, Prog. Org. Coat. 2, 81-98 (1973/74).

11. M. S. Edwards, B. R. Rodgers, and R. Salmon, Coal Technology Program, Supporting Research and Development on Separations Technology, Phase I Report, ORNL/TM-4801 (March 1975).

12. B. R. Rodgers and S. Katz, Supporting Research and Development on Separations Technology, Phase II Report: Scouting Experiments, ORNL/TM-4968 (October 1975).

13. B. R. Rodgers, S. Katz, and P. R. Westmoreland, Supporting Research and Development on Separations Technology: Final Report, ORNL/TM-5843 (October 1977).

14. A. Kitahara, T. Fujii, and S. Katano, Chem. Soc. Jpn. 44, 3242-45 (1971).

15. B. V. Derjaguin and L. Landau, Acta Phys. Chem., VRSS, 14, 633 (1941).

16. H. C. Parreira, J. Electroanal. Chem. 25, 69-78 (1970).

17. K. E. Lewis and G. D. Parfitt, Trans. Faraday Soc. 62(521), 1652-61 (May 1966).

18. O. B. E. Garner, C. W. Nult, and M. F. Mohtodi, J. Inst. Pet. 38, 986-97 (1952).

19. H. Koelmans and J. T. G. Overbeek, Discuss. Faraday Soc. 18, 52-63 (1954).

20. M. J. Mima, H. Schultz, and W. E. McKinstry, Pittsburgh Energy Research Center, PERC/R1-76/6 (September 1976).

21. A. Einstein, Am. Physik, 4(19), 289 (1906); 34, 591 (1911); Kalloid - Z 27, 137 (1920).

22. H. R. Kruyt, Colloid Science, vol. 1, Elsevier, New York, 1952.

23. R. A. Meyer, J. H. Crawford, and R. E. Tatum, "Deep-Bed Sand Filter at Savannah River Lab," Proceedings of the 13th AEC Air Cleaning Conference, Aug. 12-15, 1974.

24. C. N. Davies, Air Filtration, Academic Press, New York, 1973.

25. P. M. Heertjes and C. F. Lerk, Trans. Inst. Chem. Engrs. 45, T129-137 (1967).

26. H. F. Bogardus, R. C. Clark, J. K. Thompson, and G. H. Fielding, "Enhancement of Filter Media Performance by Corona-Free Electric Fields," Proceedings of the 13th AEC Air Cleaning Conference, Aug. 12-15, 1974.

27. V. Havlicek, Int. J. Air Water Pollut. 4(3/4), 225-6 (1961).

28. A. A. Kirsch, Aerosol Sci. 3, 25-29 (1972).

29. R. D. Rivers, ASHRAE J. 37-40 (February 1962).

30. S. P. Moulik, F. C. Cooper, and M. Bier, J. Colloid Interface Sci. 24, 427 (1967).

31. J. D. Henry, Jr., L. F. Lawler, and C. H. A. Kuo, AIChE J. 23(6), 851 (1977).

32. H. A. Pohl, J. Appl. Phys. 22(7), 869 (1951).

33. G. Zebel, J. Colloid Sci. 20, 522 (1965).

34. O. Levenspiel, Chemical Reaction Engineering, 2d ed, Chap. 9, Wiley, New York, 1972.

35. R. S. Cherry, A. C. Sharon, and Z. P. Chen, Parameters Influencing Dispersion in a Three-Phase Fluidized Bed, ORNL/MIT-254 (May 1977).

36. C. D. Scott et al., Experimental Engineering Sect. Semiannu. Prog. Rep. (Excluding Reactor Programs), Mar. 1, 1975, to Aug. 31, 1975, ORNL/TM-5291 (September 1976).

37. C. Y. Wen and Y. H. Yu, "Mechanics of Fluidization," Chem. Eng. Prog. Symp. Ser. 62, 100 (1966).

38. V. K. Bhatia and N. Epstein, "Three-Phase Fluidization: A Generalized Wake Model," p. 380 in Proceedings International Symposium on Fluidization and Its Applications, Cepadues Editions, Toulouse, 1974.

39. P. N. Bruce and L. Revel-Chion, "Bed Porosity in Three-Phase Fluidization," Powder Technol. 10, 243 (1974).

40. P. Dakshinamurty, V. Subrahmanyam, and J. N. Rao, "Bed Porosities in Gas-Liquid Fluidization," Ind. Eng. Chem. Proc. Des. Dev. 10(3), 322 (1971).

41. G. I. Efremov and I. A. Vakhrushev, "A Study of the Hydrodynamics of Three-Phase Fluidized Beds," Int. Chem. Eng. 10(1), 37 (1970).

42. S. D. Kim, C. G. J. Baker, and M. A. Bergougnou, "Phase Holdup Characteristics of Three-Phase Fluidized Beds," Can. J. Chem. Eng. 53, 134 (1975).

43. M. L. Michelsen and K. Ostergaard, "Holdup and Fluid Mixing in Gas-Liquid Fluidized Beds," Chem. Eng. J. 1, 37 (1970).

44. K. Ostergaard, "On Bed Porosity in Gas-Liquid Fluidization," Chem. Eng. Sci. 20, 165 (1965).

45. K. Ostergaard and M. L. Michelsen, "Holdup and Axial Dispersion in Gas-Liquid Fluidized Beds," Preprint 31d, 2nd Joint AIChE-IIQPR Meeting, Tampa, Florida, May 19-22, 1968.

46. K. Ostergaard and P. I. Thiesen, "The Effect of Particle Size and Bed Height on the Expansion of Mixed Phase (Gas-Liquid) Fluidized Beds," Chem. Eng. Sci. 21, 413 (1966).

47. G. R. Rigby and C. E. Capes, "Bed Expansion and Bubble Wakes in Three-Phase Fluidization," Can. J. Chem. Eng. 48, 343 (1970).